Paper ID: 164

Atomistic Investigation of Mechanical Properties of Metals Reinforced with Central and Auxiliary Voids

Mezbah Ahmed Tusar[1], Anshu Raj[2], M. Abrar Muhit[1], Abrar Faiyad[3]
[1] Department of Mechanical Engineering, Bangladesh University of Engineering and Technology
[2] School of Aerospace and Mechanical Engineering, University of Oklahoma
[3] Department of Mechanical Engineering, University of California Merced
E-mail: 1810090@me.buet.ac.bd

Abstract

Incorporation of void geometry inside solid structures can introduce interesting attributes to the mechanical characteristics of materials. The present study employs Molecular Dynamics simulations to investigate the mechanical properties of metal (Ni, W, Ti) cubes with central and auxiliary voids. Pristine structures and structures with central void alone were tested along with auxiliary voids of different sizes and positions to establish a comparative analysis. LAMMPS was used to simulate uniaxial tensile tests at different strain rates and temperatures. The results show that the ultimate tensile strength can increase with the optimum size and position of auxiliary voids as compared to cubes with a central void alone under a certain temperature range. We also found the strain rates responsible for maximum tensile strength for the optimized geometry of each metal. This study can contribute to cost-effective designing in manufacturing and it is the first numerical study to optimize auxiliary voids.

Keywords: Auxiliary voids, tensile test, Molecular Dynamics, optimized geometry.

1. Introduction

Voids frequently occur in irradiation-induced microstructures, making an accurate estimation of their strengthening impact essential for assessing material stress under irradiation conditions. Scattergood et al. [1] computed the strengthening effect of voids using advanced dislocation theory methods, incorporating dislocation self-interaction and elastic anisotropy. Their findings indicated that voids behave as substantial obstacles to dislocation motion, with void bypassing stress approaching the Orowan stress for impenetrable barriers under similar states. Osetsky [2] produced comparable findings through Molecular Dynamics (MD) simulations, also showing that tungsten possesses a considerably higher critical resolved shear stress (CRSS) than that caused by voids in iron.. Recently, Mei et al. [3] conducted molecular simulations to examine the interplay between an stretched edge dislocation and an collection of microvoids in a Face Centered Cubic (FCC) CoCrFeCuNi high entropy alloy (HEA), and they proposed a CRSS model required for dislocation to bypass voids created by irradiation in this alloy. Chen et al. [4] demonstrated that, in comparison to circular voids, flat polygonal voids result in a greater value of critical resolved shear stress because of more severe dislocation withdrawal resulting from the unique shape.

Vacancies or voids in 2D materials have been shown to enhance mechanical properties. Nahid et al. [5] offered a maneuver to enhance the fracture strength of silicene nanosheets that already have existing cracks by introducing secondary cracks symmetrically and orthogonally to the primary crevice, utilizing a mechanism they termed the "failure shielding mechanism". The existence of secondary cracks was found to significantly alter the stress allocation at the ends of the main crevice for loads applied along both armchair and zigzag directions. Dastider et al. [6] studied the increase of elastic constants at different defect percentages. The strengthening effect of voids opens up the possibility to intentionally incorporating voids in metal structures to reduce material usage.

Modern fabrication techniques like Electromigration and manufacturing techniques like Focused Ion Beam (FIB) Melting now allow us to artificially introduce voids of different sizes at different positions inside metal products. Latz et al. [7] and Sindermann et al. [8] have extensively shown how electromigration influences the formation and propagation of voids. Additionally, Li et al. [9] demonstrated the effect of electric fields on dislocation motion. These precedents allow us to conclude that controlling the size and position of voids inside a 3D structure is, in fact, possible. Håkonsen et al. [10] showed a maneuver to create voids of preferred dimensions at preferred positions through milling and melting during metal product manufacturing.

Although previous studies investigated the effects of voids, a quantitative study on optimizing the geometry and positioning of the voids is absent. In our research, we used molecular dynamics simulations to investigate the mechanical properties of three different metals, varying the size and position of voids. Since several manufacturing processes leave defects in the final product, which result in reduced mechanical properties, the ability to mitigate the negative impacts of existing voids with planned incorporation of auxiliary voids can open up a possibility to further improve the quality of products that undergo neutron and heavy-ion irradiation.

2. Methodology

Large-scale Atomic/Molecular Massively Parallel Simulator (LAMMPS) was chosen to carry out the MD simulations imperative to our study. The embedded atom method (EAM) was employed to compute the pairwise interactions among atoms. For EAM potential, the total energy E_i of an atom i is calculated by:

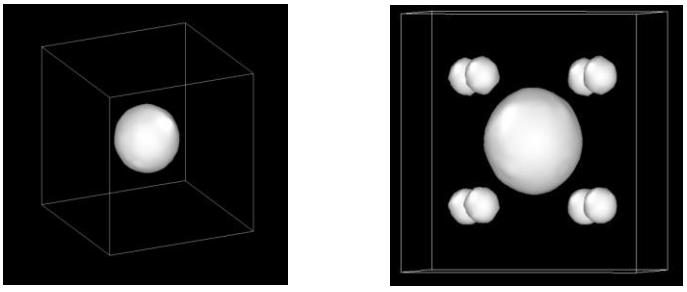
$$E_i = F_\alpha \left(\sum_{j \neq i} \rho_\beta(r_{ij})\right) + \frac{1}{2}\sum_{j \neq i} \phi_{\alpha\beta}(r_{ij}) \quad (1)$$

where F represents the embedding energy, dependent on the atomic electron density ρ; φ denotes the pair potential interaction; α and β indicate the types of atoms of atoms i and j. The multi-body characteristic of the EAM potential arises from the embedding energy term. Both summations in the equation encompass all neighboring atoms j of atom i within a defined cutoff distance. Using this potential, we first calculated the stress-strain relations for pristine structures, the results of which show convincing similarity with existing literature.

Metal cubes have been prepared with an approximate length of 126Å on each side. Lattice constants used for Nickel (FCC), Tungsten (BCC) are 3.52 Å, 3.165 Å respectively. For Titanium (HCP), lattice parameters are employed as a = 2.95Å and c = 4.68Å. This resulted in atom numbers 186624, 128000, and 116100 in Ni, W, and Ti, respectively. All cubes are configured with the x, y, and z axes oriented along the [100], [010], and [001] crystallographic directions, respectively. At first, energy was minimized in pristine cubes by applying an external stress tensor. This enables the box dimensions to adjust throughout minimizing iterations, ensuring that final configuration achieves both a potential energy minimum for the atoms and a system pressure tensor that closely aligns with the specified external tensor. Atom coordinates were also iteratively adjusted to minimize the energy with a stopping tolerance for the energy of 1^{-30} eV and a stopping tolerance for the force of 1^{-30} eV/ Å. After the initial minimization, voids were created in pristine structures (demonstrated in Fig. 1), which led to 7 different geometries to work with. Central void has a radius of 25.421 Å. The position and size of auxiliary voids are summarized in Table 1. Throughout the paper, the nomenclature declared in Table 1 is followed.

Table 1. Types of Void Geometry

Type	Auxiliary Void Position (distance of auxiliary void from cube surface/length of cube)	Void Size (radius of auxiliary void/radius of central void)
Type 1 (pristine)	0	0
Type 2 (only central void)	0	0
Type 3	0.2	1/2
Type 4	0.2	1/3
Type 5	0.2	1/5
Type 6	0.3	1/3
Type 7	0.3	1/5



(a) (b)

Fig. 1. A cubic shape with (a) central void, (b) both central and auxiliary voids

After the creation of voids, the system's energy was minimized using the NVE ensemble over a duration of 5 ps. Additionally, the Nose-Hoover thermostat and barostat were used for 50 ps in order to equilibrate the temperature and pressure, respectively. Ultimately, uniaxial strain is applied in the z-direction at a constant rate, which is parameterized to determine the rate's impact on strength. The tensile test is performed under the NVT ensemble utilizing the Nose-Hoover thermostat. Every deformation simulation is performed up to failure. Stress values were determined by computing the per-atom stress tensor for each atom.

3. Results & Discussions

Effect of Void Size and Position

The stress-strain curves for various types of Ni cubes under uniaxial tension are presented in Fig. 2. As demonstrated in Fig. 2 (a), at 300k temperature, ultimate tensile strength shows 0.26% increase for Type 4 (distance of auxiliary void from cube surface = 0.2*total length & central void to auxiliary void ratio = 5) cube structure as compared to Type 2 (without any auxiliary void). At 600k, we see 2.35% increase in UTS for Type 7 (distance of auxiliary void from cube surface = 0.25*total length & central void to auxiliary void ratio = 5) cube structure. At 900k, no improvement is observed with the incorporation of auxiliary voids as depicted in Fig. 2(c). Fig. 3 presents the stress-strain relations for different types of W cubes under uniaxial tension. At 300k, Ultimate Tensile Strength shows an increase of 1.6429% for Type 7 (distance of auxiliary void from cube surface = 0.25*total length & central void to auxiliary void ratio = 5) cube structure as compared to Type 2 (without any auxiliary void). At 600k, Ultimate Tensile Strength shows 10.08% increase for Type 6 (distance of auxiliary void from cube surface = 0.25*total length & central void to auxiliary void ratio = 3) cube structure with respect to Type 2. At 900k, no improvement is observed with the incorporation of auxiliary voids. The stress-strain relations for different types of Ti cubes under uniaxial tension are shown in Fig. 4. At 300k, Ultimate Tensile Strength shows 0.2% increase for Type 4 (distance of auxiliary void from cube surface = 0.2*total length & central void to auxiliary void ratio = 5) cube structure as compared to Type 2 (without any auxiliary void). At 600k, Ultimate Tensile Strength shows a 7.1% increase for Type 5 (distance of auxiliary void from cube surface = 0.25*total length & central void to auxiliary void ratio = 3) cube structure with respect to Type 2.

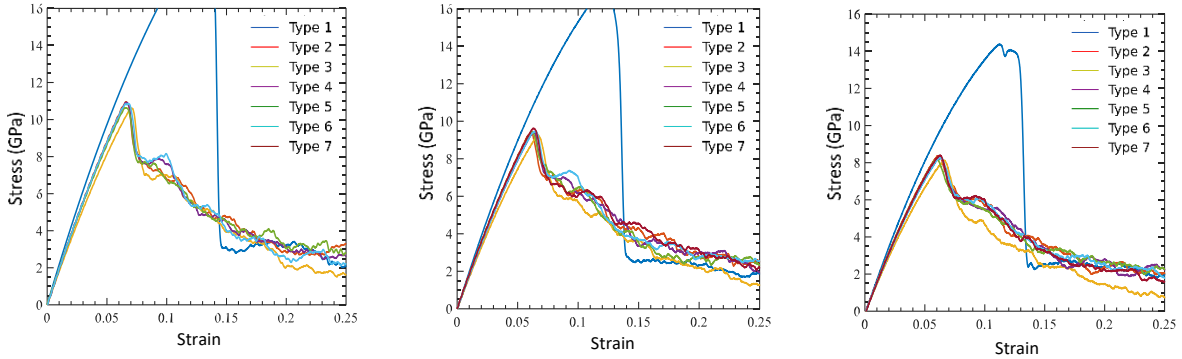


Fig. 2. Variation of stress with strain in nickel cubes at (a) 300K, (b) 600k, and (c) 900k temperature

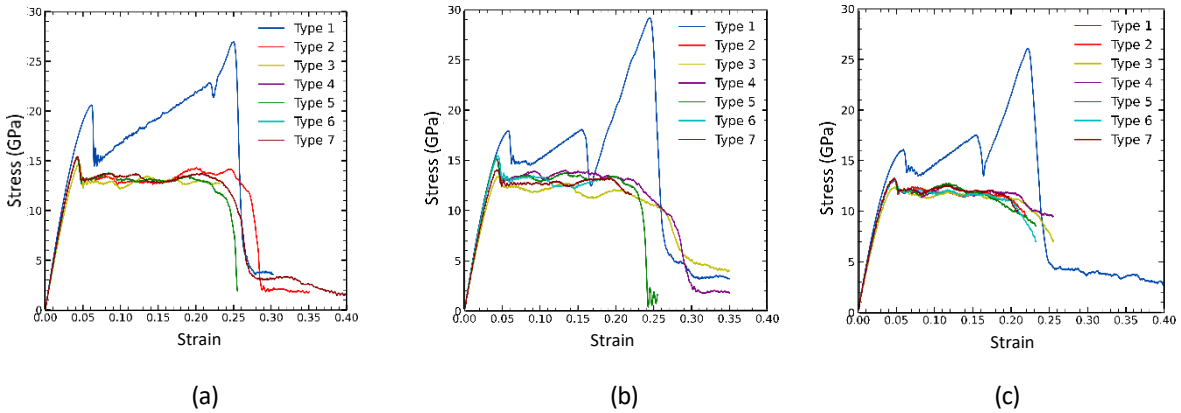


Fig. 3. Variation of stress with strain in tungsten cubes at (a) 300K, (b) 600k, and (c) 900k temperature

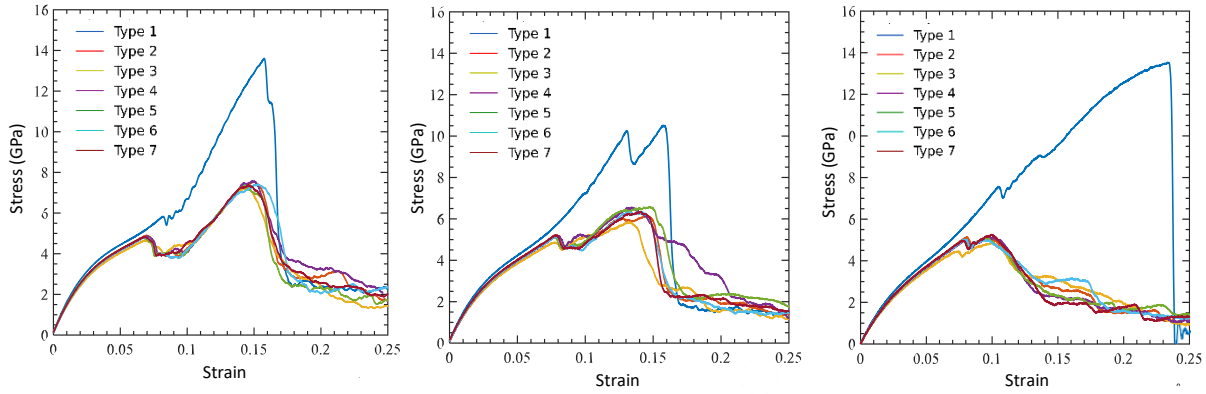


Fig. 4. Variation of stress with strain in titanium cubes at (a) 300K, (b) 600k, and (c) 900k temperature

For the first time at 900k, we observed an improvement with the incorporation of auxiliary voids. The ultimate tensile strength of Ti at 900k increased up to 2.236% for Type 7 (distance of auxiliary void from cube surface = 0.25*total length & central void to auxiliary void ratio = 5) cube structure with respect to Type 2. The aforementioned results imply that the optimum void geometry is material specific, i.e., there is no single geometry that ensures the maximum strength for all materials and all temperatures. This happens due to the different lattice structures of the materials we have tested. Type 7 is found to be optimum for the highest number of cases (3 out of 9) and shows promising improvements in other cases as well.

Effect of Temperature

For every single material, we found the greatest improvement in strength for 600k temperature. As depicted in Fig. 5, at room temperature (300k), Nickel and Tungsten show the second highest improvement, as opposed to Titanium, which shows little deviation. On the other hand, Titanium shows significant improvement at 900k, but Nickel and Tungsten have none.

Effect of Strain Rate

Various strain rates were tested on a single type of void geometry (distance of auxiliary void from cube surface = 0.2*total length & central void to auxiliary void ratio = 5) at 300k temperature. Fig. 6 shows the resulting stress-strain relations for each material. A strain rate of 0.012 ps^{-1} yields a maximum strength of 13.7 GPa for Nickel and 18.3 GPa for Tungsten. For Titanium, a strain rate of 0.006 ps^{-1} yields a maximum strength of 8.7 GPa with 0.012 ps^{-1}, which closely approximates the same value. Hence, it is evident that higher strain rates result in higher strength.

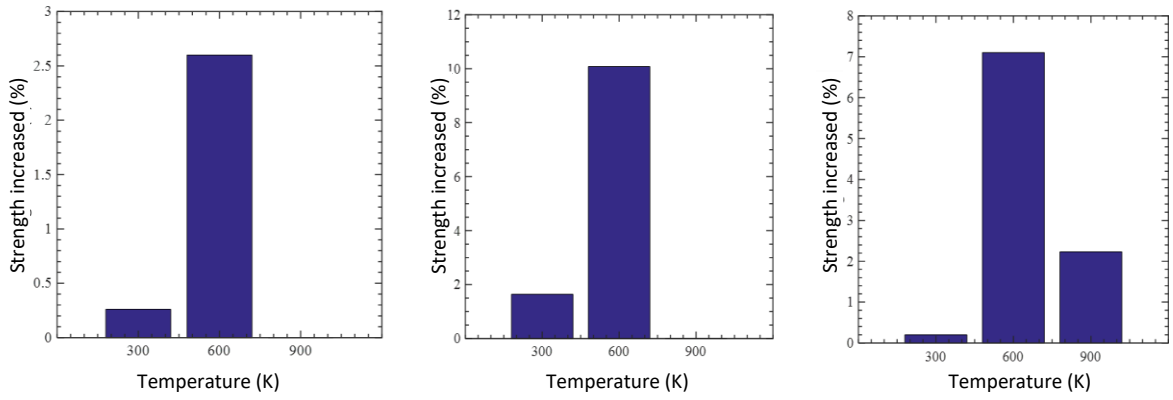


Fig. 5. Variation of increase in strength with the incorporation of auxiliary voids in (a) nickel, (b) tungsten, and (c) titanium cubes at different temperatures

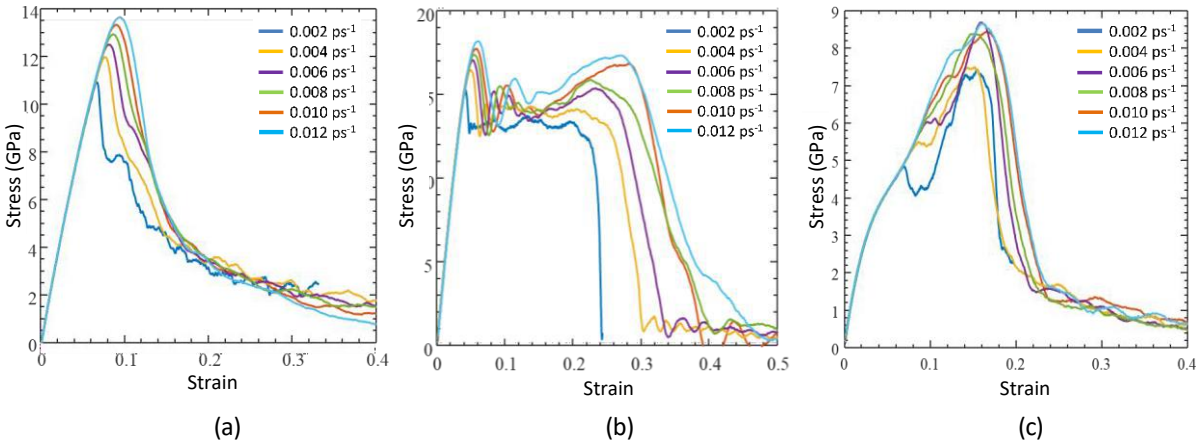


Fig. 6. Variation of stress with strain at different strain rates in (a) nickel, (b) tungsten, and (c) titanium cubes at 300k temperature

4. Conclusion

We investigated the effects of void size, position, strain rate, and temperature on the tensile property of cubic structures composed of nickel (Ni), tungsten (W), and titanium (Ti). The findings reveal that the introduction of auxiliary voids can improve UTS, but the optimal void geometry is material-specific and temperature-dependent. For Ni, W, and Ti, void geometries with auxiliary voids positioned 0.25 times the total cube length from the surface and a central void to auxiliary void ratio of 5 (Type 7) generally yield the best results. However, the magnitude of improvement varies: W shows the most significant increase in strength at 600K with Type 6, while Ti benefits from Type 7 at 900K. Overall, the results indicate that no single void geometry maximizes UTS across all materials and temperatures, due to differences in lattice structure. Type 7 performs well in several cases, making it a promising design for multiple conditions. The study also shows that temperature plays a critical role in UTS improvements, with 600K yielding the greatest increases for all materials, while auxiliary voids offer little to no benefit at 900K for Ni and W. Additionally, higher strain rates consistently enhance UTS across all tested materials, with Ni and W showing the highest strengths at a strain rate of 0.012 ps^{-1}. In conclusion, the interplay between void geometry, material properties, temperature, and strain rate is complex, and optimizing these parameters can significantly enhance mechanical performance. These findings provide valuable insights for designing materials with improved tensile strength, particularly in high-temperature applications.

5. References

[1] R.O. Scattergood, D.J. Bacon, "The strengthening effect of voids," *Acta Metall.*, vol. 30, no. 8, pp. 1665–1677, Aug. 1982.

[2] Y. N. Osetsky, "Atomic-scale mechanisms of void strengthening in tungsten," *Tungsten*, vol. 3, pp. 65-71, 15 March 2021.

[3] X. Mei, Y. Xu, Y. Zhu, L. Zhao, Z. Li, M. Huang, "The statistic and fluctuant phenomena of interaction between edge extended dislocation and microvoid in FCC CoCrFeCuNi high entropy alloy," *J. Nucl. Mater.*, vol. 568, p. 153884, Sep. 2022.

[4] Y. Chen, Y. Liu, Q. Fang, J. Li, Y. Liu, P. K. Liaw"An unified model for dislocations interacting with complex-shape voids in irradiated metals," *Int. J. Mech. Sci.*, vol. 185, p. 105689, Nov. 2020.

[5] S. M. Nahid, S. Nahian, M. Motalab, T. Rakib, S. Mojumder, and M. M. Islam, "Tuning the mechanical properties of silicene nanosheet by auxiliary cracks: a molecular dynamics study," *RSC Adv.*, vol. 8, no. 53, pp. 30354–30365, 2018.

[6] A. G. Dastider, A. Rasul, E. Rahman, and Md. K. Alam, "Effect of vacancy defects on the electronic and mechanical properties of two-dimensional $MoSi_2N_4$," *RSC Adv.*, vol. 13, no. 8, pp. 5307–5316, 2023.

[7] A. Latz, S. Sindermann, L. Brendel, G. Dumpich, F.-J. Meyer zu Heringdorf, and D. E. Wolf, "Simulation of electromigration effects on voids in monocrystalline Ag films," *Phys. Rev. B*, vol. 85, no. 3, p. 035449, Jan. 2012.

[8] S. P. Sindermann, A. Latz, G. Dumpich, D. E. Wolf, and F.-J. Meyer zu Heringdorf, "Lattice dependent motion of voids during electromigration," *J. Appl. Phys.*, vol. 113, no. 13, p. 134505, Apr. 2013, doi: 10.1063/1.4798367.

[9] M. Li *et al.*, "Harnessing dislocation motion using an electric field," *Nat. Mater.*, pp. 1–6, Jun. 2023.

[10] V. Håkonsen, G. Singh, J. He, and Z. Zhang, "Focused ion beam milling of self-assembled magnetic superstructures: an approach to fabricate nanoporous materials with tunable porosity," *Mater. Horiz.*, vol. 5, no. 6, pp. 1211–1218, Oct. 2018.